2.6 High-rate precise point positioning: observation of crustal deformation by using 1-Hz GPS data

Tomoji Takasu (Technical Consultant)
ttaka@gpspp.sakura.ne.jp, URL: gpspp.sakura.ne.jp

Abstract

Seismic surface waves caused by the Sumatra-Andaman earthquake are detected by the GPS precise point positioning (PPP) technique. The precision of high-rate PPP is usually degraded by the interpolation error of low-rate satellite clocks. To solve this problem, 1-Hz satellite clocks are estimated using the high-rate observations at GPS stations worldwide. Subsequently ground motions are analyzed by kinematic-PPP using the 1-Hz satellite clocks. This technique is referred to as high-rate PPP (HR-PPP). By HR-PPP, the seismic waves generated by the earthquake can be fairly detected. In contrast to relative positioning conventionally applied to GPS kinematic analysis, HR-PPP can efficiently observe the widely distributed crustal deformations generated by an earthquake involving long-period waves. To validate HR-PPP, the analyzed displacements are compared with the seismograms. The HR-PPP solutions are in very good agreements with the integrated velocities measured using broadband seismometers nearby the GPS stations.

Keywords: Sumatra-Andaman earthquake, kinematic GPS, precise point positioning

2.6.1 Introduction

High-rate kinematic analysis coupled with global positioning system (GPS) has recently become one of the effective methods to observe the dynamic crustal deformations caused by an earthquake even within a short time frame. *Larson et al.* [2003] employed 1-Hz GPS measurements to analyze the ground surface displacements generated by the 2002 Denali fault earthquake in Alaska (Mw 7.9) and found a good agreement with the integrated strong motion records by seismic instruments. They stated that the high-frequency GPS, which has wide dynamic range and frequency bandwidth without any saturation problems, provides another important tool to study earthquakes. *Bock et al.* [2004] also demonstrated that the GPS can provide single-epoch measurements of ground motion greater than 2–3mm induced by the earthquake with dense network of 1-Hz stations.

The relative positioning, involving the construction of baselines between receivers, has been conventionally used for precise GPS kinematic analysis. Using this technique, the receiver coordinates are obtained as relative solutions to a reference station position that is usually tightly constrained to an absolute static value. It is difficult to separate the receiver motion from that of the reference station. The reference station errors like multipath effects also propagate into the relative solutions. Therefore, to analyze the ground displacement generated by a large-scale earthquake involving widely-distributed and long-duration teleseismic waves, a very long baseline of up to a few thousand kilometers is necessary to eliminate the influence of the reference station movement by the earthquake. However, a very long baseline generally degrades the positioning precision. This is primarily because there are fewer satellites in the common view of both the receiver and reference station, leading to a poor satellite-receiver geometry.

The precise point positioning (PPP) was introduced by *Zumberge et al.* [1997], as an efficient and robust analysis technique for large GPS receiver networks. PPP can estimate a single receiver position without any reference station or baseline by fixing satellite positions and clocks to previously determined values. The International GNSS Service (IGS) (http://igscb.jpl.nasa.gov) provides accurate and high-quality products including GPS satellite orbits and clocks based on the post-mission analysis of observations at more than 300 permanent stations worldwide. In many cases, the IGS products or other precise ephemerides are used as pre-determined satellite orbits and clocks for PPP. However, the IGS satellite clock products are currently provided at only 5-min intervals. The interpolation error of the low-rate clocks degrades the accuracy of high-rate PPP; this is because the instability of the onboard GPS frequency standards causes an unpredictable random drift in the satellite clock even within a short period. This is a primary problem in the application of PPP to high-rate GPS kinematic analysis to investigate seismic deformations generated by an earthquake. The satellite clock drift and interpolation error is not negligible in the case of other higher rate clock products like CODE or JPL, which provides 30-s interval solutions. Nevertheless, no sufficient high-rate satellite clocks are widely available at present for high-rate PPP.

On 26 December 2004, the Sumatra-Andaman earthquake (Mw 9.1–9.3), which is the largest seismic event on Earth in more than 40 years, produced the most devastating tsunami in recorded history and caused more than 283,000 deaths. This large-scale earthquake involved huge fault areas and large fault slips; it was began at the northwest of Sumatra at a depth of about 30 km. A rupture of the length of up to 1300 km propagated to the Andaman Islands and a short-period radiation was generated for at least 500 s. The peak-to-peak ground motion exceeded 9 cm in Sri Lanka and the long period displacements exceeded 1 cm across on earth's surface [*Lay et al.*, 2005].

This study will present the results of the GPS kinematic analysis performed by applying HR-PPP to detect the seismic waves widely distributed along the earth's surface generated by the Sumatra-Andaman earthquake.

2.6.2 Analysis Strategy

In this study, to avoid the satellite clock interpolation error problem, a two-step procedure is employed for the high-rate PPP. In the first step, 1-Hz precise satellite clocks are determined by using high-rate GPS observation data obtained from globally distributed receivers with precise satellite orbits and low-rate clocks. In the second step, high-rate ground displacements are analyzed by the kinematic-PPP using these 1-Hz satellite clocks obtained in the first step. The author refers this strategy as high-rate precise point positioning (HR-PPP).

The ionosphere-free linear combination (LC) of the dual-frequency carrier-phase GPS observables is expressed as follows in units of m [*Kouba*, 2003b] :

$$L = \rho + c(dt - dT) + T + N + \Delta + \varepsilon \qquad (1)$$

where ρ is the geometric distance between the satellite and the receiver, dt and dT are the receiver and satellite clock-bias, respectively, and c is the speed of light in vacuum. T is the tropospheric delay, N is the carrier-phase ambiguity of ionosphere-free LC, and ε is the measurement error including the station multipath effect. The term Δ represents the sum of precise corrections such as satellite and receiver antenna phase-center offset and variation, site displacements by earth tides and phase-windup effect. These corrections can not be usually neglected in an undifferenced carrier-phase measurement model for PPP. In this equation, the geometric distance ρ is computed iteratively with the satellite and receiver positions considering Earth's rotation during the signal travel time [*Leick*, 2004]. In contrast to the satellite clock, the satellite orbit can be safely interpolated onto the satellite positions at any time using high-degree polynomial without significant errors [*Schenewerk*, 2003]. The tropospheric delay T is also obtained with tropospheric zenith total delay (ZTD) and an appropriate mapping function.

For the first-step of the HR-PPP, the 5-min interval solutions of the receiver positions, ZTDs and carrier-phase ambiguities are determined by conventional static-PPP with 5-min interval satellite clocks and 15-min interval orbits provided by IGS. Once these low-rate solutions are obtained, higher rate values can be acquired by a simple linear interpolation of these values, wherein they are assumed to be stable for a short period. By fixing the terms of ρ, T and N of the equation with these interpolated solutions, the clock bias dt and dT of all the satellites and receivers can be estimated in a least-square manner using the one epoch measurements acquired from many globally distributed receivers. For the estimation, the constraint of a reference receiver's clock bias equal to zero is added to avoid a rank-deficient problem.

In December 2004, the IGS had been operating over 50 high-rate stations providing 1-Hz or 0.1-Hz sampling GPS observation data. These include the proposed IGS sites. The observation data of the IGS stations had been uploaded to and archived in the Crustal Dynamics Data Information System (CDDIS, ftp://cddis.gsfc.nasa.gov). Figure 1 shows the location of these stations. In this study, to determine the 1-Hz satellite clocks, a total of 50 stations were selected from all the sites. Some ill-conditioned stations with a large multipath, high measurement noises, or frequent cycle-slips were excluded.

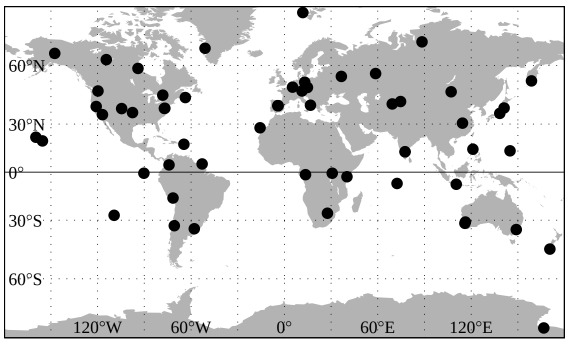

Figure 1. Location of high-rate IGS stations providing 1-Hz or 0.1-Hz GPS observation data in December 2004

For the 1-Hz clock estimation, the IGS final products, that have a formal accuracy <5 cm as the satellite position and <0.1 ns as the satellite clock bias, were used as precise GPS satellite orbits and clocks. The high-rate satellite positions were obtained by 10th-degree Lagrange interpolation of the 15-min interval values provided as the IGS final orbit. The other estimation models and setting of precise corrections are summarized in Table 1.

Figure 2 shows the GPS satellite clock stability as Allan deviation for an averaging time of 1–10000 s, which are derived from the estimated 1-Hz clocks in the period of 0:00:00–23:59:59 GPST, 25 December 2004. The estimated satellite clocks are relative solutions with respect to the reference AMC2 Hydrogen Maser (HM) atomic clock. The stability of the reference clock is below 10^{-13} at 10000 s. Note that the high-frequency stability of the estimated satellite clock is affected slightly by the receiver noises or station multipath effects.

According to the GPS satellite clock stability, the maximum interpolation error is approximated to be 0.1–0.3 ns (3–9 cm) for 5-min interval clocks and 0.01–0.03 ns (3–9 mm) for 30-s interval clocks. Clearly, the low-rate clock interpolation error for high-rate positioning can not be neglected as compared to the raw kinematic-PPP precision, which is typically less than 1 cm and 3 cm in the horizontal and vertical positions, respectively, for a short period. The interpolation error could adversely affect the positioning precision for observation of high-frequency receiver movements.

Table 1. Detailed models and settings of precise corrections for the 1-Hz satellite clock estimation and kinematic-PPP.

Item	Models/Settings
Parameter estimator	Extended Kalman filter (EKF, forward/backward) and fixed interval smoother. [*Gelb et al.*, 1974]
A priori tropospheric delay	Saastamoinen model
Tropospheric mapping function	GMF [*Boehm et al.*, 2006]
Process-noise of tropospheric parameters	ZTD: 10^{-4} m/sqrt(s) Gradients: 10^{-5} m/sqrt(s),
Satellite/receiver antenna phase-center offset and variation	IGS_05.ATX (IGS absolute antenna PCV models)
Site displacement by earth-tides	Solid earth tide: IERS Conventions 1996 ch. 7 Step 1 and Step 2 K1 only Ocean loading: NAO.99b (GOTIC2) Pole tide: IERS Conventions 1996 ch. 7
Phase-windup effect	*Wu et al.*, [1996]
Reference frame	ITRF2000 [*Altamimi et al.*, 2002]

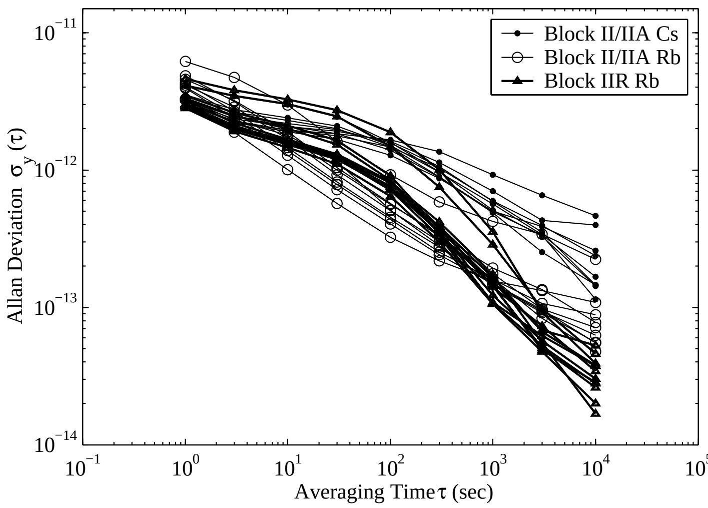

Figure 2. Allan deviation plots of the GPS satellite clocks for an averaging time of 1–10000 s. They are derived from 50 high-rate IGS station observations in 0:00:00–23:59:59 GPST on 25 December 2004. The estimated satellite clocks are referenced to the AMC2 HM atomic clock.

Kouba [2003a] also presented the capability of 1-Hz kinematic PPP to detect seismic waves induced by large earthquakes. He used the interpolated IGS satellite clocks for PPP. He concluded that the 5-min sampling of the IGS clocks appears to be sufficient even for the high frequency position solutions with cm resolutions. However, in the station position solutions with the interpolated clocks, obvious common mode drifts, which might be caused by the clock interpolation error, appeared especially in the vertical component. The IGS 5-min sampling clocks seem to be insufficient to observe dynamic ground motions with high-rate PPP and higher-rate clocks are necessary.

In the second step of HR-PPP, the high-rate receiver coordinates are estimated by the general PPP procedure using the high-rate GPS observation data, the precise satellite orbits and the 1-Hz satellite clocks from the first step. In this study, extended Kalman filter (EKF) formulation is employed as the parameter estimator. In this scheme, the time variation of a receiver's position is modeled as a white-noise stochastic process; here, at each epoch the receiver's position is assumed to be independent adjacent epochs and no correlation exists between them, i.e., pure kinematic receiver position model. The tropospheric ZTD and horizontal gradient parameters are also modeled as random-walk stochastic processes, respectively. Further, the carrier-phase ambiguity is modeled as constant state in an arc. In contrast to the double-differenced measurements for relative positioning, the undifferenced carrier-phase ambiguity for PPP has no integer characteristics because of the satellite's and receiver's instrumental biases. These biases are hardly separatable from the satellite and receiver clock bias; therefore, they can not be resolved into integer solutions. Consequently, the carrier-phase ambiguities are estimated as float values. Once a cycle-slip is detected, the parameter is re-initialized to an approximated value. Additionally, the prefit and postfit residual tests are implemented for quality control. If a residual exceeds the appropriate threshold, the observation datum is excluded and the re-estimation process runs without all the outliers. The other detailed setting and correction models are the same as those shown in Table 1 for the 1-Hz satellite clock estimation.

The sidereal filtering concept was suggested by *Bock et al.* [1991] and was modified by *Choi et al.* [2004] by considering the satellite repeating time offset to a sidereal day. This technique utilizes the high correlation between the residuals of the estimated receiver positions at intervals of a sidereal period (23 h 56 min 4 s). It is particularly effective in the high-rate GPS kinematic analysis of a ground-fixed receiver coordinate to reduce both the high-frequency noises and low-frequency undulations. In this study, the modified sidereal filter is applied to the HR-PPP results coupled with a previous day's solution.

2.6.3 Results and Considerations

All the features described above are implemented in the GPS/GNSS precise analysis software package GpsTools [*Takasu et al.*, 2005], which the author has been developing. The following analysis results were obtained with GpsTools ver. 0.6.2.

By using the 1-Hz HR-PPP technique, the high-rate coordinates of all the continuously operating high-rate IGS stations are estimated in the period of 0:00:00–2:59:59 GPST on 26 December 2004.

The displacements of these stations could affect the clock estimation and appear as noises of the estimated 1-Hz satellite clocks. As for the Sumatra-Andaman earthquake, many of the worldwide GPS stations were shaken by the seismic wave. In order to reduce the noise of the estimated 1-Hz satellite clocks, the observation data in the period with a peak-to-peak displacement of over 4 cm were rejected after all the station coordinates were analyzed with the HR-PPP. The 1-Hz satellite clocks were estimated again without these noise sources and the final HR-PPP analysis was performed with the re-estimated satellite clocks. The difference between the first estimated and the re-estimated clocks are reached to 0.1 ns (3 cm) at the maximum.

The estimated ground displacements of the 14 stations where the seismic surface waves by the Sumatra-Andaman earthquake are fairly detected are plotted in Figure 3. The locations of these stations and the epicenter are also plotted in Figure 4. Only a modified sidereal filter is applied using the previous day's solution. The offset of the repeating period of a satellite to a sidereal day is set to –9 sec. The cut-off frequency of the low-pass filter for the previous day residuals is also set to 0.05 Hz. The displacement plots in Figure 3 are arranged in the order of increasing the distance from the epicenter of the earthquake.

As shown in Figure 3, at IISC, Bangalore India, the largest seismic ground movement began at 1:08 GPST and its peak-to-peak amplitude of north-south displacement exceeded 15 cm. The other sites also clearly captured the teleseismic waves propagating and spreading along the earth surface from the epicenter. Even at CHUR, Churchill, Canada, beyond 13000 km from the epicenter, the horizontal seismic wave can be observed after 1:46 GPST. However, the vertical ground displacements at some stations such as FAIR and NYA2 are contaminated by high-frequency noises; therefore, the vertical seismic waves are hardly distinguishable from the noises. It is considered that these noises are due to the poor satellite-receiver geometry and the station multipath

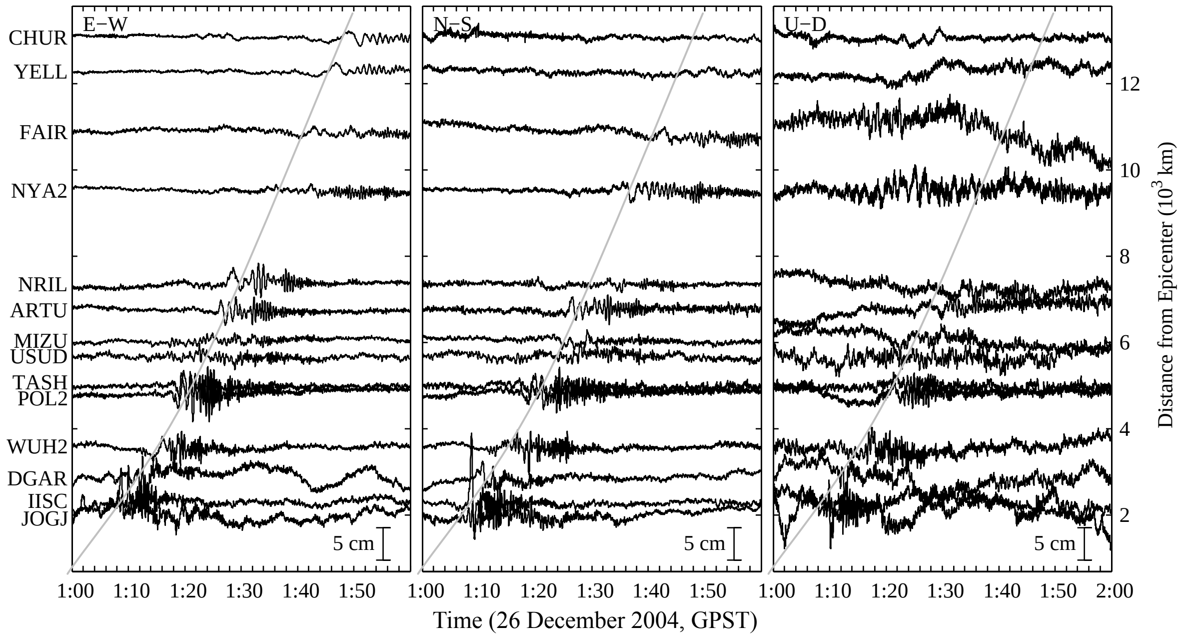

Figure 3. East-west (left), north-south (center) and up-down (right) components of the ground displacements at the GPS stations observed by the 1-Hz HR-PPP, in the time frame of 1:00–2:00 GPST on 26 December 2004. Only a sidereal filter using the previous day's residuals is applied. The stations aligned according to the distance from the epicenter of the Sumatra-Andaman earthquake. Gray lines indicate approximated surface wave (3.4–4.2 km/s) propagation time.

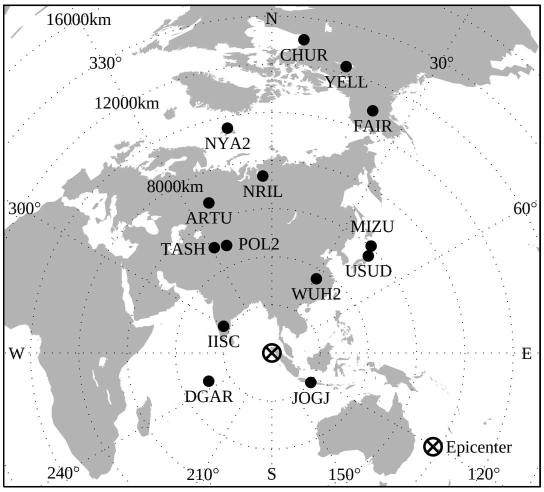

Figure 4. GPS station locations, azimuth angles, and distances from the epicenter of the Sumatra-Andaman earthquake (3.308N, 95.874E).

effects.

The large rupture process of the Sumatra-Andaman earthquake began at 0:59:12 GPST. The propagation speed of the Rayleigh wave generated by the earthquake is approximated to be 3.4–4.2 km/s based on the HR-PPP analysis results. *Ammon et al.* [2005] suggested that the amplitudes of the Rayleigh waves of the earthquake are enhanced along the rupture direction at around an azimuth angle of 330˚ for 150-s to 300-s period waves. The high-rate GPS sites with relatively large teleseismic deformations are concentrated at the azimuth angle of 300˚–360˚ from the epicenter. This fact is consistent with the rupture direction of the earthquake.

International Deployment of Accelerometers (IDA), which is an element of Incorporated Research Institutions for Seismology (IRIS) Global Seismographic Network (GSN), has been deploying broadband and very-long-period seismometers worldwide (http://ida.ucsd.edu). To validate the analysis results with the HR-PPP, the estimated ground motions generated by the earthquake are compared with the displacements derived from the integration of the raw ground velocities observed at the IRIS/IDA sites in the vicinity of the GPS stations. All of these velocities are measured using a very broadband seismometer (Streckeisen STS-1). The long-period seismic instrument has a nearly flat response to the ground velocity from 0.1 s to 360 s period.

Figure 5 shows the comparison of the seismic waves observed by HR-PPP with the integrated seismograms record at the IRIS/IDA sites. These

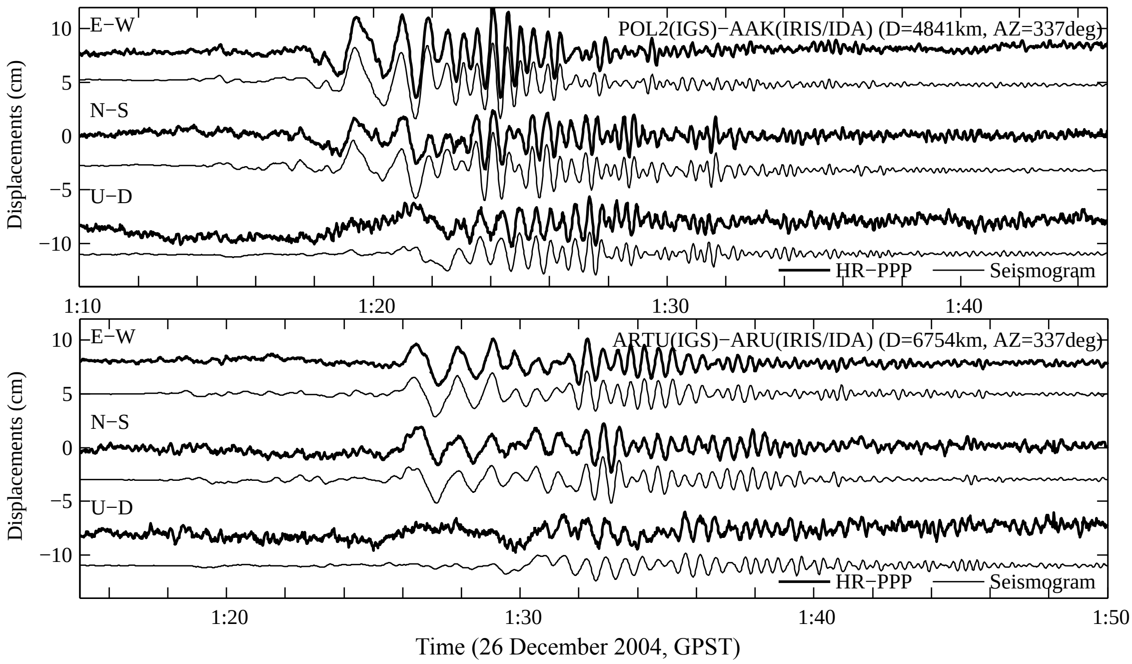

Figure 5. Comparisons of the observed seismic waves with the displacements as the integrated velocities measured using broadband seismometers nearby the GPS stations. The upper plot shows POL2 (IGS) and AAK (GSN-IRIS/IDA) and the lower one shows ARTU (IGS) and ARU (GSN-IRIS/IDA). The geographic distance between POL2 and AAK is 17.1 km and that between ARTU and ARU is 0.3 km. Only a sidereal filter using the previous day's data is applied to the HR-PPP results. No bandpass filter is applied to either of the displacements.

comparisons are among the POL2 (IGS) and AAK (IRIS/IDA) at Bishkek in Kyrghyzstan, and ARTU (IGS) and ARU (IRIS/IDA) at Arti in Russia. As shown in Figure 5, the seismic waves observed by HR-PPP, which seems to include the direct body wave (P and S wave) leading to the surface waves, are in a very good agreement with the displacements recorded by the seismometers with regard to both the amplitude and phase. However, a slight difference is found with regard to high-frequency noises, especially those of the vertical component, which might be caused by the station multipath effects of the GPS carrier-phase observables. Additionally, the noises in the satellite clocks, derived from the high-rate clock estimation process, could also responsible be for the high-frequency differences.

Figure 6 shows the analyzed seismic waves at another site–DGAR at the Diego Garcia Island in the Indian Ocean. The displacements are separated according to the frequency ranges using bandpass filters. In this figure, a large difference can be seen between the HR-PPP result and the seismograph below 0.003 Hz. The response of the seismometer in this low-frequency range is insufficient; therefore, it is difficult to capture the displacements properly. In contrast, the bandwidth of the kinematic GPS is sufficient to detect the low-frequency deformations. However, the long-period noises originated from systematic errors like tropospheric correction residuals and imperfect antenna phase-center models are included in the solutions obtained from the GPS kinematic analysis. *Ohta et al.* [2006] analyzed the power-spectrum of the kinematic GPS time series obtained from the very long baseline relative positioning using GIPSY/OASIS II. They concluded that the sensitivity of kinematic GPS is slightly insufficient to detect very-long-period displacements. Therefore, it is difficult to judge whether the displacements below 0.003 Hz recorded by HR-PPP represents true seismic waves or only low-frequency noises of the GPS kinematic analyses. For HR-PPP as well as the other GPS kinematic analyses, future research and development are necessary to elucidate the sources of the long-period errors and enhance the positioning technique.

2.6.4 Conclusions

The application of HR-PPP, which is a new kinematic GPS analysis strategy involving the 1-Hz satellite clock estimation and high-rate single point precise positioning, to detect the seismic waves caused by the Sumatra-Andaman earthquake is

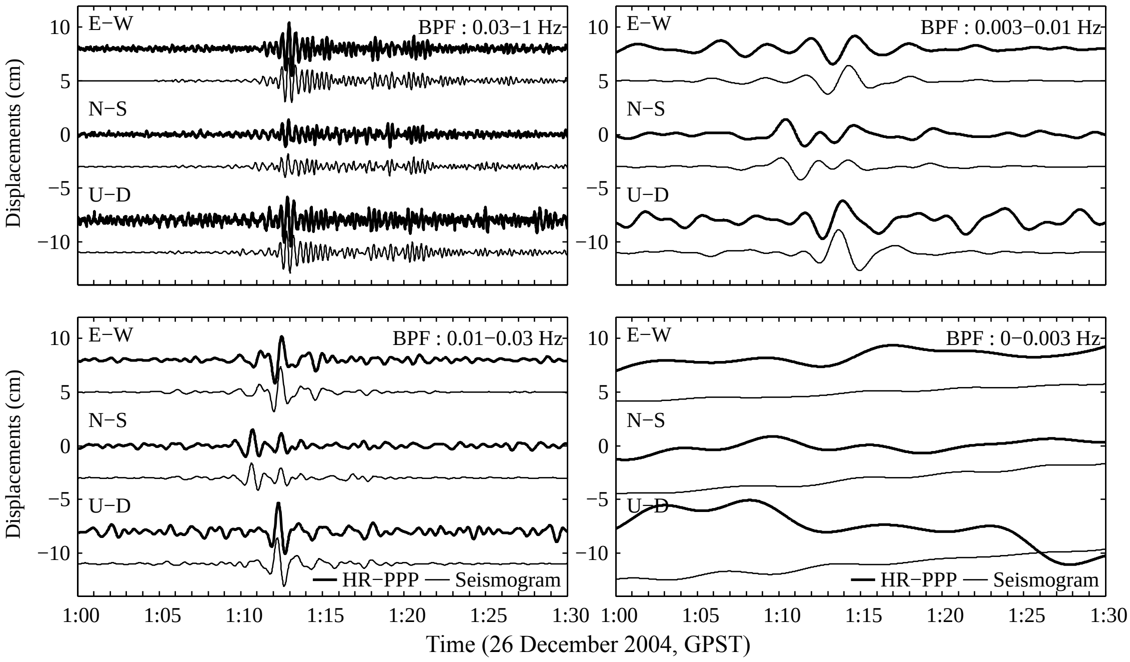

Figure 6. Bandpass-filtered displacement obtained by HR-PPP and by the seismometer at DGAR (IGS, GSN-IRIS/IDA). Signal pass frequencies are 0.03–1 Hz (upper-left), 0.01–0.03 Hz (lower-left), 0.003–0.01 Hz (upper-right), and 0–0.003 Hz (lower-right). At this site, the difference between HR-PPP and seismograph reading are remarkable at low-frequencies, below 0.003 Hz.

demonstrated. HR-PPP can reasonably detect the teleseismic deformations generated by an earthquake at the GPS stations worldwide. The ground displacements analyzed by HR-PPP are in a very good agreement with the integrated velocities measured using the broadband seismometers installed near the GPS sites. As compared to conventional relative kinematic GPS technique, HR-PPP without the influence of the reference station and baseline provides a more effective method to investigate a large-scale earthquake. With the current GPS kinematic analysis, the long-period noises frequently appear even in the HR-PPP solutions. Future research and development are necessary to enhance this technique.

Acknowledgments

The author is grateful to Mr. Yusaku Ohta (Nagoya University) and an anonymous reviewer for the very useful comments to the manuscript. The author is also grateful to IGS for providing high-quality products and high-rate GPS observation data recorded at many stations worldwide.

References

Altamimi, Z., P Sillard, and C. Boucher (2002), ITRF2000: A new release of the International Terrestrial Reference Frame for earth science applications, *Journal of Geophysical Research*, *107* (B10), 2214, doi:10.1029/2001JB0000561

Ammon, C. J., Chen Ji, H-K. Thio, D. Robinson, S. Ni, V. Hjorleifsdottir, H. Kanamori, T. Lay, S. Das, D. Helmberger, G. Ichinose, J. Polet, and D. Wald (2005), Rupture process of the 2004 Sumatra-Andaman Earthquake, *Science, 308*, 1133–1139

Bock, Y. (1991), Continuous monitoring of crustal deformation, *GPS World*, *2*(6), 40–47

Bock, Y., L. Prawirodirdjo, and T. I. Melbourne (2004), Detection of arbitrarily dynamic ground motions with a dense high-rate GPS network, *Geophys. Res. Lett.*, *31*, L06604, doi 10.1029/2003GL019150

Boehm, J., A. Niell, P. Tregoning, and H. Schuh (2006), Global Mapping Function (GMF): A new empirical mapping function based on numerical weather model data, *Geophys. Res. Lett., 33*, L07304, doi:10.1029/2005GL025546.

Choi, K., A. Bilich, K. M. Larson, and P. Axelrad (2004), Modified sidereal filtering: Implications for high-rate GPS positioning, *Geophys. Res. Lett., 31,* L22608, doi: 1029/2004GL021621

Gelb, A., J. F. Kasper, Jr., R. A. Nash, Jr., C. F. Price, and A. A. Sutherland, Jr. (1974), Applied Optimal Estimation, The M. I. T. Press, Cambridge, Massachusetts, and London, England

Kouba, J. (2003a), Measuring seismic waves induced by large earthquakes with GPS, *Stud. Geophys. Geod.*, *47*, 741–755

Kouba, J. (2003b), A Guide to using International GPS Service (IGS) products, ftp://igscb.jpl.nasa.gov /igscb/resource/pubs/GuidetoUsingIGSProdcts.pdf

Larson, K. M., P. Bodin, J. Gomberg (2003), Using 1-Hz GPS data to measure deformations caused by the Denali fault earthquake, *Science, 300,* 1421–1424

Lay, T., H. Kanamori, C. J. Ammon, M. Nettles, S. N. Ward, R. C. Aster, S. L. Beck, S L. Bilek, M. R. Brudzinski, R. Butler, H. R. DeShon, G. Ekström, K. Satake, and S. Sipkin (2005), The great Sumatra-Andaman earthquake of 26 December 2004, *Science, 308*, 1127–1133

Leick, A. (2004), GPS Satellite Surveying, 3rd Edition, John Wiley & Sons, Inc., Hoboken, New Jersey, USA

McCarthy, D. D. (1996), IERS Technical Note 21, IERS Conventions 1996

Ohta, Y., I. Meilano, T. Sagiya, F. Kimata, and K. Hirahara (2006), Large surface wave of the 2004 Sumatra-Andaman earthquake captured by the very long baseline kinematic analysis of 1-Hz GPS data, *Earth Planets Space, 58,* 153–157

Schenewerk, M. (2003), A breaf review of basic GPS orbit interpolation strategies, *GPS Solutions*, *6*, 265-267, doi: 10.1007/s10291-002-0036-0

Takasu, T., and S. Kasai (2005), Development of precise orbit/clock determination software for GPS/GNSS, the 49th Space Sciences and Technology Conference, Hiroshima, Japan (in Japanese)

Wu, J.T., G. A. Hajj, W. I. Bertiger and S. M. Lichten (1993), Effects of antenna orientation on GPS carrier phase, *Manuscripta Geodaetica*, *18*, 91–98

Zumberge, J. F., M. B. Heflin, D. C. Jefferson, and M. M. Watkins and F. H. Webb (1997), Precise point positioning for the efficient and robust analysis of GPS data from large networks, *Journal of Geophysical Research, 102* (B3), 5005–5017